A new family of covalent inhibitors block nucleotide binding to the active site of pyruvate kinase

Published in final edited form as:
Biochem J. 2012 November 15; 448(1): 67–72. doi:10.1042/BJ20121014.

A new family of covalent inhibitors block nucleotide binding to the active site of pyruvate kinase

Hugh P. Morgan[*], **Martin J. Walsh**[†], **Elizabeth A. Blackburn**[*], **Martin A. Wear**[*], **Matthew B. Boxer**[†], **Min Shen**[†], **Iain W. Mcnae**[*], **Matthew W. Nowicki**[*], **Paul A. M. Michels**[‡], **Douglas S. Auld**[†], **Linda A. Fothergill-Gilmore**[*], and **Malcolm D. Walkinshaw**[*,1]

[*]Centre for Translational and Chemical Biology, School of Biological Sciences, University of Edinburgh, Michael Swann Building, The King's Buildings, Mayfield Road, Edinburgh EH9 3JR, UK

[†]NIH Chemical Genomics Center, NIH Center for Translational Therapeutics, National Human, Genome Research Institute, National Institutes of Health, 9800 Medical Center Drive, Rockville, MD 20850, U.S.A

[‡]Research Unit for Tropical Diseases, de Duve Institute and Laboratory of Biochemistry, Université catholique de Louvain, Avenue Hippocrate 74, B-1200 Brussels, Belgium

SYNOPSIS

Pyruvate kinase (PYK) plays a central role in the metabolism of many organisms and cell types, but the elucidation of the details of its function in a systems biology context has been hampered by the lack of specific high-affinity small molecule inhibitors. High-throughput screening has been used to identify a family of saccharin derivatives which inhibit *Leishmania mexicana* PYK (*Lm*PYK) activity in a time- (and dose-) dependent manner; a characteristic of irreversible inhibition. The crystal structure of 4-[(1,1-dioxo-1,2-benzothiazol-3-yl)sulfanyl]benzoic acid (DBS) complexed with *Lm*PYK shows that the saccharin moiety reacts with an active-site lysine residue (Lys335), forming a covalent bond and sterically hindering the binding of ADP/ATP. Mutation of the lysine residue to an arginine residue eliminated the effect of the inhibitor molecule, providing confirmation of the proposed inhibitor mechanism. This lysine residue is conserved in the active sites of the four human PYK isoenzymes, which were also found to be irreversibly inhibited by DBS. X-ray structures of PYK isoforms show structural differences at the DBS binding pocket, and this covalent inhibitor of PYK provides a chemical scaffold for the design of new families of potentially isoform-specific irreversible inhibitors.

Keywords

Leishmania mexicana; lysine covalent modification; nucleotide binding; pyruvate kinase; saccharin analogues; covalent inhibitor

INTRODUCTION

Pyruvate kinase (PYK) catalyses the last step in glycolysis to produce ATP and pyruvate, and in most organisms studied, PYKs have similar homotetrameric architectures with each

[1]To whom correspondence should be addressed: Centre for Translational and Chemical Biology, School of Biological Sciences, The University of Edinburgh, Michael Swann Building, The King's Buildings, Mayfield Road, Edinburgh EH9 3JR, UK. Tel.: 44 (0) 131 650 7056; m.walkinshaw@ed.ac.uk.

The atomic co-ordinates of the *Lm*PYK-DBS structure have been deposited in the PDB under code 3SRK.

monomer composed of four domains (Figure 1a). Four human tissue-specific PYK isoenzymes have been described: *Hs*RPYK (erythrocyte), *Hs*LPYK (liver), *Hs*M1PYK (muscle) and *Hs*M2PYK (embryonic or tumour). The M1 isoform is constitutively active while the other three are allosterically regulated by the effector molecule fructose 1,6-bisphosphate (F16BP) [1]. Trypanosomatid PYKs are distinguished by their use of the chemically distinct molecule fructose 2,6-bisphosphate (F26BP) as the effector, and recently the detailed allosteric mechanism for PYK of the pathogenic protist *Leishmania mexicana* (*Lm*PYK) has been elucidated [2].

PYK has been implicated as playing a central role in a number of proliferative and infectious diseases, and the discovery of isoenzyme-specific inhibitors or activators of PYK could be of potential interest in the elucidation of the etiology of cancer [3] and of metabolic diseases such as diabetes and obesity [4], as well as infectious diseases caused by bacteria [5], trypanosomatid parasites [6] and the malaria parasites *Plasmodium* spp. [7]. For example, PYK deficiency in erythrocytes results in nonspherocytic haemolytic anemia and over 130 mutations in *Hs*RPYK have been identified which contribute to the disease [8, 9]. There is also a strong link between the up-regulation of the human M2PYK isoenzyme and oncogenesis [3], and this isoenzyme is found in all tumours studied to date [3]. The effector-regulated *Hs*M2PYK can facilitate a build-up of phosphometabolites which are required for the cancer cell to proliferate. A number of potent activators of *Hs*M2PYK have been identified with AC_{50} values around 30 nM [10], however the only examples of *Hs*M2PYK inhibitors bind relatively weakly with IC_{50} values of 10 to 20 μM [11].

RNAi knockdown of PYK and other enzymes in the glycolytic pathway in trypanosomatids has facilitated a systems biology approach to elucidate the roles played by these enzymes [12]. A complementary approach to regulate PYK activity by small molecule compounds has been hindered by the lack of appropriate chemical tools. One of the few compounds currently available is the polysulfonated drug suramin, one of the earliest synthetic drugs used to treat human African trypanosomiasis. It is a promiscuous binder with a complex pharmacology and poorly understood mode of action. However, it has been shown to inhibit seven of the ten enzymes in the glycolytic pathway of *Trypanosoma brucei* [13, 14]. A crystal structure of a complex of *Lm*PYK with suramin shows that it acts as an ATP/ADP mimic and binds competitively with the ADP substrate [15]. Suramin also inhibits all four human isoforms of PYK with K_i values between 1 and 20 μM [15]. In addition, affinity labelling of rabbit-muscle PYK has been achieved by covalent modification of active-site residues using nucleotide analogues [16] [17]. The only other known general PYK inhibitor is the substrate analogue oxalate, which exhibits poor specificity and binds with relatively weak affinity (K_i = 220 μM) [18]. Selective inhibitors of PYK are needed as biochemical tools for studying the glycolytic pathway and as potential leads for drug development. Here we report the discovery of a novel covalent PYK inhibitor, 4-[(1,1-dioxo-1,2-benzothiazol-3-yl)sulfanyl]benzoic acid (DBS, Figure 1c).

EXPERIMENTAL

Expression and purification of wild-type and Lys335Arg mutant forms of *Lm*PYK

Chemically competent *Escherichia coli* Rosetta 2* (DE3)pLysS (Merck – Cat. No. 71403) cells were transformed with either the wild-type or mutated plasmid (see Supplementary data). Both wild-type and Lys335Arg mutant forms of *Lm*PYK were expressed and purified as described previously [15].

Synthesis and characterization of covalent inhibitors

A series of saccharin derivatives identified as inhibitors of *Lm*PYK by quantitative high-throughput screening (qHTS) was further elaborated by *de novo* chemical synthesis,

purification and characterization. The procedures for the synthesis and purification of compounds NCG00186526, NCGC00059857, NCGC00188411 and NCGC00188636 (Figure 1c) and their characterization are described in detail in the Supplementary data. One of these analogues, DBS (NCGC00188636), displayed improved stability and solubility profiles relative to the original screening hit (NCGC00186526) and was therefore used for the experiments described in this paper.

PYK inhibitor assay

The following reagents were added to a 50 mL Falcon tube (equivalent to 11×1 mL assays): 8.58 mL of assay mix (1x assay buffer (50 mM triethanolamine (TEA), pH 7.2, 100 mM potassium chloride, 3 mM magnesium chloride, 10% glycerol), 0.2 mM NADH (128023-Roche), 3.2 U/mL lactate dehydrogenase (Sigma-61309)), 1.6 U/mL *Lm*PYK, 0.4 mM phosphoenolpyruvate (PEP) (Sigma- 79430) and 2.20 mL of 250 μM inhibitor solution (made up with 1x assay buffer from a 170 mM stock in 100% DMSO, final conc. 50 μM – added last to the reaction mix). The control reaction mix was made identically except 1x buffer was used in place of the inhibitor solution. Both the control and inhibitor reaction mixtures were incubated throughout the experiment in a 25 °C water bath (prior to the addition of inhibitor which was also incubated at 25 °C). To 990 μL of the reaction mix, 10 μL of 20 mM ADP (final concentration = 0.2 mM ADP (Sigma-A4386); made up with 1x assay buffer) was added to start the reaction. The mixture was gently agitated and the decrease in absorbance at 340 nm was measured for 2 min (using Lambda Bio). The process was repeated every 20 min over 200 min for both the control and inhibitor. The initial rate was then calculated using UV kinlab. The rate for each inhibitor assay was expressed as a percentage of the control assay.

Preparation of inhibitor-modified *Lm*PYK

The DBS inhibitor (Stock = 172 mM in 100% dimethylsulfoxide (DMSO)) was added to 200 μL of *Lm*PYK (10 mg/mL: 184 μM in 20 mM TEA buffer (pH 7.2) and 10% glycerol) to a final concentration of 9 mM (maintaining a similar molar ratio of inhibitor to protein as used in the kinetic assay). The sample was then incubated overnight at 4 °C. Dithiothreitol (DTT) was added to a final concentration of 1 mM, and the *Lm*PYK-DBS inhibitor mix was incubated at room temperature for 15 min. The DTT and leaving group were removed by repeated dilutions (using 20 mM TEA buffer (pH 7.2) and 10% glycerol) and by concentrating the sample in a Vivaspin column (molecular mass cut off = 100 kDa). The sample was concentrated to 12 mg/mL.

Crystallization and data collection

Samples of inhibitor-modified *Lm*PYK (prepared as described) were diluted to 10 mg/mL using a buffer containing 20 mM TEA (pH 7.2) and 1,3,6,8-pyrenetetrasulfonic acid (PTS, final concentration 1 mM). Single crystals of inhibitor-modified *Lm*PYK complexed with PTS were obtained at 4 °C by vapour diffusion using the hanging drop technique. The drops were formed by mixing 1.5 μL of protein solution with 1.5 μL of a well solution, composed of 12 – 16% polyethyleneglycol (PEG) 8,000, 20 mM TEA buffer (pH 7.2), 50 mM magnesium chloride, 100 mM potassium chloride and 10% glycerol. The drops were equilibrated against a reservoir filled with 0.5 mL of well solution. Crystals grew to maximum dimensions (1.0×0.2×0.1 mm) after 24 – 48 h. Prior to data collection, crystals were equilibrated for 14 h over a well solution composed of 14 – 18% PEG 8,000, 20 mM TEA buffer (pH 7.2), 50 mM magnesium chloride, 100 mM potassium chloride and 25% glycerol, which eliminated the appearance of ice rings. Intensity data were collected (φscans were 2° over 180°) at the Diamond synchrotron radiation facility in Oxfordshire, United Kingdom on beamline IO3 from a single crystal cryocooled in liquid nitrogen. A single crystal gave data to a resolution of 2.65 Å at 100 K.

Structure determination and analysis of model geometry

The *Lm*PYK-DBS structure was solved and refined using the method described previously [2], yielding R/R_{free} values of 21.9/27.35. A further round of TLS restrained refinement (four optimal TLS groups were determined using TLSMD procedure [19]) yielded final R/R_{free} values of 22.3/26.6. The geometry of the model was assessed using MolProbity [20]. Although electron density was well defined for Thr296 (a key active-site residue), it exhibits geometry outwith the Ramachandran plot here and in many PYK structures. This is primarily due to a restricted geometry, which facilitates interactions with active-site ligands.

RESULTS AND DISCUSSION

High-throughput screening identified a series of saccharin-based inhibitors

There were 292,740 compounds in the NIH Molecular Libraries-Small Molecule Repository tested in the primary screen for the wild-type *Lm*PYK (PubChem AID 1721). The screen was performed at seven compound concentrations using quantitative high-throughput screening (qHTS) [21, 22] and identified 1,087 high-quality concentration-response curves, corresponding to a hit rate of 0.4% of the library. One of the top actives from this series was the saccharin derivative NCGC00186526, with an IC_{50} of 10 μM. The oxo linkage in this compound was labile, and the molecule was found to hydrolyse to saccharin and the corresponding phenol (Figure 1c). Stable sulphur (NCGC00188411) and nitrogen (NCGC00059857) analogues were prepared (Figure 1c) and tested in the *Lm*PYK activity assay. Only NCGC00188411 showed inhibitory activity (IC_{50} = 5 μM). At this point it was hypothesized that covalent modification of either cysteine or lysine in the enzyme, as well as the leaving group ability of the resultant phenol, thiophenol and aniline explained the trend in activity [23]. The sulphur analogue (4-[(1,1-dioxo-1,2-benzothiazol-3-yl)sulfanyl]benzoic acid (DBS, NCGC00188636, Figure 1c and 1d) was used in subsequent experiments.

Covalent modification of LmPYK by DBS is confirmed by X-ray crystal structure analysis

*Lm*PYK crystals grown in the presence of 2 mM oxalate and 2.8 mM DBS (*Lm*PYK-OX/DBS) were anisotropic, and diffracted poorly to approximately 4 Å. Despite the relatively low resolution, difference (F_o-F_c) electron density was observed near Lys335 in all active sites (Figure 1b) suggesting that Lys335 was covalently modified by the saccharin moiety (Figure 1d). Improved quality crystals diffracting to 2.65 Å were obtained using a purification protocol of DBS-modified *Lm*PYK in which DMSO was removed by dilution and PTS was added to the crystallization solution (see Table 1 for data collection and refinement statistics). Electron density corresponding to the covalent addition of the saccharin moiety to Lys335 is clearly visible in all active sites (Figure 1b). The modified Lys335 residue is located at the adenine-binding site and blocks ADP/ATP binding (Figure 2a). Electron density was carefully examined around all other lysines in the structure but no evidence for their covalent modification was observed.

Inhibition of LmPYK by DBS is time dependent

An inhibition assay was used to examine the covalent reaction further, whereby *Lm*PYK activity was monitored over time in the presence of 50 μM DBS (Figure 3d). Maximal inhibition of ~80% was achieved after ~250 min (Figure 1e, curve A), although *Lm*PYK inhibition never reached 100% inhibition even after 10 h (after prolonged incubation periods at 25 °C both the wild-type and Lys335Arg of *Lm*PYK mutant began to aggregate). The small amount of remaining activity could possibly be due to weak binding of ADP to the DBS-modified active site. The X-ray structure of the modified enzyme suggests that the saccharin group covalently bound to Lys335 with its flexible side chain could adopt conformations that would still allow ADP access to the active site (Figure 2a), albeit with

reduced affinity. In terms of potential antiparasitic activity it is relevant to note that incomplete depletion (about 75%) of the intracellular concentration of PYK by RNAi is sufficient to cause cell death in the pathogenic bloodstream form of *T. brucei* [24].

The Lys335Arg mutation confirms the covalent inhibitory mechanism

To test whether inhibition stems from the covalent modification of Lys335 and not modification of other lysine residues in PYK, we expressed and purified the Lys335Arg mutant of *Lm*PYK. The wildtype and Lys335Arg mutant of *Lm*PYK enzymes exhibited similar activity and kinetic parameters (Supplementary Table S1). However, on addition of DBS and under identical assay conditions to that of wild-type *Lm*PYK, the Lys335Arg mutant exhibited essentially no change in activity over time (Figure 1e, curve D).

Evidence of selectivity of DBS for Lys335 is suggested by the inability of DBS to inhibit rabbit lactate dehydrogenase (a coupling enzyme) through covalent modification of a similar active-site lysine, Lys56. This residue is similar in both location (found also on the rim of the active site cleft) and interaction (interacting with the ribose hydroxyl of the nucleoside group of NAD) to Lys335 of *Lm*PYK (Supplementary Figure S3). A lysine residue (Lys531) also exists in the active site of firefly luciferase (PDB code 2DIT). Both these coupling enzymes provide good controls to suggest that DBS displays selectivity for binding Lys335. The X-ray structural results discussed in the following section provide a rationale for this specificity.

Mechanism of covalent modification by DBS is suggested by the structure of LmPYK-suramin

A series of phenyl sulfonated dye-like molecules including the trypanocidal drug suramin has been shown to bind in a near-identical position within the active site of *Lm*PYK [15]. The *Lm*PYK-DBS monomer was superimposed onto the *Lm*PYK-suramin structure, with excellent alignment of the protein backbones (RMS fit = 0.5 Å). Modelling a fit of the sulfonamide group of the unreacted DBS molecule onto the sulfone group in the suramin complex, perfectly positions Lys335 for nucleophilic attack on C3 of the saccharin ring to release the sulphide moiety (Figures 1d, 2). The requirement for DBS to dock in such a specific pose could explain its specificity for Lys335 over other lysine residues in the structure. The X-ray structure however suggests that once the covalent bond has formed, the modified lysine adopts a different pose. Comparisons of the relevant X-ray structures show the sulphone groups of suramin and of the saccharin moiety of DBS covalently attached to Lys335 are 4.4 Å apart (Figure 2b and Supplementary Figure S3).

DBS is a covalent inhibitor of both human and trypanosomatid PYKs

Lysine 335 is relatively well conserved among different PYK species and it is of interest that naturally occurring mutations in *Hs*RPYK (equivalent residue Lys410) to either glutamic acid [9] or aspartic acid [25] result in non-spherocytic haemolytic anaemia. DBS was found to inhibit both *Hs*RPYK (the human PYK isoenzyme present in erythrocytes) and *Hs*M2PYK (the human PYK isoenzyme present in embryonic and tumour cells) with IC_{50} values of 8 μM and 16.3 μM, respectively (see Supplementary Figure S4). These values compare with an IC_{50} value of DBS for *Lm*PYK of 2.9 μM. Modelled poses of the pre-cleavage DBS binding pocket highlight sequence differences between the trypanosomatid and human enzymes (Figure 2d) and it is likely that such differences in the saccharin binding pocket provide an opportunity for the design of more potent species-specific inhibitors against either trypanosomatid or human PYK isoforms.

Supplementary Material

Refer to Web version on PubMed Central for supplementary material.

Acknowledgments

We thank Paul Shinn, Danielle VanLeer, Thomas Daniel, Christopher LeClair and James Bougie for assistance with compound management and purification. We would also like to thank the staff at the Diamond synchrotron radiation facility in Oxfordshire, United Kingdom.

FUNDING

This research was supported in part by the Molecular Libraries Initiative of the NIH Roadmap for Medical Research and the Intramural Research Program of the National Human Genome Research Institute, National Institutes of Health. Additional funding was from the MRC, and the European Commission through its INCO-DEV programme. The Centre for Translational and Chemical Biology and the Edinburgh Protein Production Facility were funded by the Wellcome Trust and the BBSRC.

Abbreviations used

DBS	4-[(1,1-dioxo-1,2-benzothiazol-3-yl)sulfanyl]benzoic acid, compound number NCGC00188636
DEAE	diethylaminoethyl
DMF	*N,N*-dimethylformamide
DMSO	dimethylsulfoxide
DTT	dithiothreitol
EDTA	ethylenediaminetetraacetic acid
ESI-MS	electrospray ionization mass spectrometry
Et_3N	triethylamine
F16BP	fructose 1,6-bisphosphate
F26BP	fructose 2,6-bisphosphate
HPLC	high-performance liquid chromatography
***Hs*PYK**	human pyruvate kinase
***Hs*RPYK**	human erythrocyte PYK
***Hs*LPYK**	human liver PYK
***Hs*M1PYK**	human muscle PYK
***Hs*M2PYK**	human embryonic or tumour PYK
***Lm*PYK**	*Leishmania mexicana* PYK
MLSMR	Molecular Libraries Small Molecule Repository
PEG	polyethyleneglycol
PEP	phosphoenolpyruvate
PTS	1,3,6,8-pyrenetetrasulfonic acid
PYK	pyruvate kinase
qHTS	quantitative high-throughput screening
TEA	triethanolamine

TFA trifluoroacetic acid

REFERENCES

1. Fothergill-Gilmore LA, Michels PA. Evolution of glycolysis. Prog. Biophys. Mol. Biol. 1993; 59:105–235. [PubMed: 8426905]
2. Morgan HP, McNae IW, Nowicki MW, Hannaert V, Michels PA, Fothergill-Gilmore LA, Walkinshaw MD. Allosteric mechanism of pyruvate kinase from *Leishmania mexicana* uses a rock and lock model. J Biol. Chem. 2010; 285:12892–12898. [PubMed: 20123988]
3. Christofk HR, Vander Heiden MG, Harris MH, Ramanathan A, Gerszten RE, Wei R, Fleming MD, Schreiber SL, Cantley LC. The M2 splice isoform of pyruvate kinase is important for cancer metabolism and tumour growth. Nature. 2008; 452:230–233. [PubMed: 18337823]
4. Vander Heiden MG, Cantley LC, Thompson CB. Understanding the Warburg Effect: the metabolic requirements of cell proliferation. Science. 2009; 324:1029. [PubMed: 19460998]
5. Zoraghi R, Worrall L, See RH, Strangman W, Popplewell WL, Gong H, Samaai T, Swayze RD, Kaur S, Vuckovic M, Finlay BB, Brunham RC, McMaster WR, Davies-Coleman MT, Strynadka NC, Andersen RJ, Reiner NE. Methicillin-resistant *Staphylococcus aureus* (MRSA) pyruvate kinase as a target for bis-indole alkaloids with antibacterial activities. J. Biol. Chem. 2011; 286:44716–44725. [PubMed: 22030393]
6. Nowicki MW, Tulloch LB, Worralll L, McNae IW, Hannaert V, Michels PAM, Fothergill-Gilmore LA, Walkinshaw MD, Turner NJ. Design, synthesis and trypanocidal activity of lead compounds based on inhibitors of parasite glycolysis. Bioorg. Med. Chem. 2008; 16:5050–5061. [PubMed: 18387804]
7. Ayi K, Min-Oo G, Serghides L, Crockett M, Kirby-Allen M, Quirt I, Gros P, Kain KC. Pyruvate kinase deficiency and malaria. N Engl J Med. 2008; 358:1805–1810. [PubMed: 18420493]
8. Zanella A, Bianchi P, Fermo E. Pyruvate kinase deficiency. Haematologica. 2007; 92:721–723. [PubMed: 17550841]
9. Zanella A, Fermo E, Bianchi P, Valentini G. Red cell pyruvate kinase deficiency: molecular and clinical aspects. British J Haematol. 2005; 130:11–25.
10. Jiang J, Boxer MB, Heiden MGV, Shen M, Skoumbourdis AP, Southall N, Veith H, Leister W, Austin CP, Park HW. Evaluation of thieno [3, 2-b] pyrrole [3, 2-d] pyridazinones as activators of the tumor cell specific M2 isoform of pyruvate kinase. Bioorg. Med. Chem. Lett. 2010; 20:3387–3393. [PubMed: 20451379]
11. Vander Heiden MG, Christofk HR, Schuman E, Subtelny AO, Sharfi H, Harlow EE, Xian J, Cantley LC. Identification of small molecule inhibitors of pyruvate kinase M2. Bioccem. Pharmacol. 2009; 79:1118–1124.
12. Verlinde C, Hannaert V, Blonski C, Willson M, Périé JJ, Fothergill-Gilmore LA, Opperdoes FR, Gelb MH, Hol WGJ, Michels PAM. Glycolysis as a target for the design of new anti-trypanosome drugs. Drug Resistance Updates. 2001; 4:50–65. [PubMed: 11512153]
13. Willson M, Callens M, Kuntz DA, Perié J, Opperdoes FR. Synthesis and activity of inhibitors highly specific for the glycolytic enzymes from *Trypanosoma brucei*. Molec. Biochem. Parasitol. 1993; 59:201–210. [PubMed: 8341319]
14. Albert MA, Haanstra JR, Hannaert V, Van Roy J, Opperdoes FR, Bakker BM, Michels PAM. Experimental and in silico analyses of glycolytic flux control in bloodstream form *Trypanosoma brucei*. J. Biol. Chem. 2005; 280:28306–28315. [PubMed: 15955817]
15. Morgan HP, McNae IW, Nowicki MW, Zhong W, Michels PAM, Auld DS, Fothergill-Gilmore LA, Walkinshaw MD. The trypanocidal drug suramin and other trypan blue mimetics are inhibitors of pyruvate kinases and bind to the adenosine site. J Biol. Chem. 2011; 286:31232–31240. [PubMed: 21733839]
16. DeCamp DL, Colman RF. Identification of tyrosine and lysine peptides labeled by 5'-p-fluorosulfonylbenzoyl adenosine in the active site of pyruvate kinase. J. Biol. Chem. 1986; 261:4499–4503. [PubMed: 3082867]

17. Vollmer SH, Walner MB, Tarbell KV, Colman RF. Guanosine 5'-O-[S-(4-bromo-2,3-dioxobutyl)]thiophosphate and adenosine 5'-O-[S-(4-bromo-2,3-dioxobutyl)]thiophosphate. New nucleotide affinity labels which react with rabbit muscle pyruvate kinase. J Biol. Chem. 1994; 269:8082–8090. [PubMed: 8132533]

18. Dombrauckas JD, Santarsiero BD, Mesecar AD. Structural basis for tumor pyruvate kinase M2 allosteric regulation and catalysis. Biochemistry. 2005; 44:9417–9429. [PubMed: 15996096]

19. Painter J, Merritt EA. Optimal description of a protein structure in terms of multiple groups undergoing TLS motion. Acta. Crystallogr. D Biol. Crystallogr. 2006; 62:439–450. [PubMed: 16552146]

20. Davis IW, Leaver-Fay A, Chen VB, Block JN, Kapral GJ, Wang X, Murray LW, Bryan Arendall Iii W, Snoeyink J, Richardson JS. MolProbity: all-atom contacts and structure validation for proteins and nucleic acids. Nucl. Acids Res. 2007

21. Inglese J, Auld DS, Jadhav A, Johnson RL, Simeonov A, Yasgar A, Zheng W, Austin CP. Quantitative high-throughput screening: a titration-based approach that efficiently identifies biological activities in large chemical libraries. Proc. Nat. Acad. Sci. 2006; 103:11473. [PubMed: 16864780]

22. Shukla SJ, Sakamuru S, Huang RL, Moeller TA, Shinn P, VanLeer D, Auld DS, Austin CP, Xia MH. Identification of clinically used drugs that activate pregnane X receptors. Drug Metab. Disp. 2011; 39:151–159.

23. Carey, FA.; Sundberg, RJ. Advanced organic chemistry: Structure and mechanisms. Springer Verlag; 2007.

24. Bakker BM, Michels PAM, Opperdoes FR, Westerhoff HV. Glycolysis in bloodstream form *Trypanosoma brucei* can be understood in terms of the kinetics of the glycolytic enzymes. J. Biol. Chem. 1997; 272:3207. [PubMed: 9013556]

25. Pendergrass DC, Williams R, Blair JB, Fenton AW. Mining for allosteric information: Natural mutations and positional sequence conservation in pyruvate kinase. IUBMB Life. 2006; 58:31–38. [PubMed: 16540430]

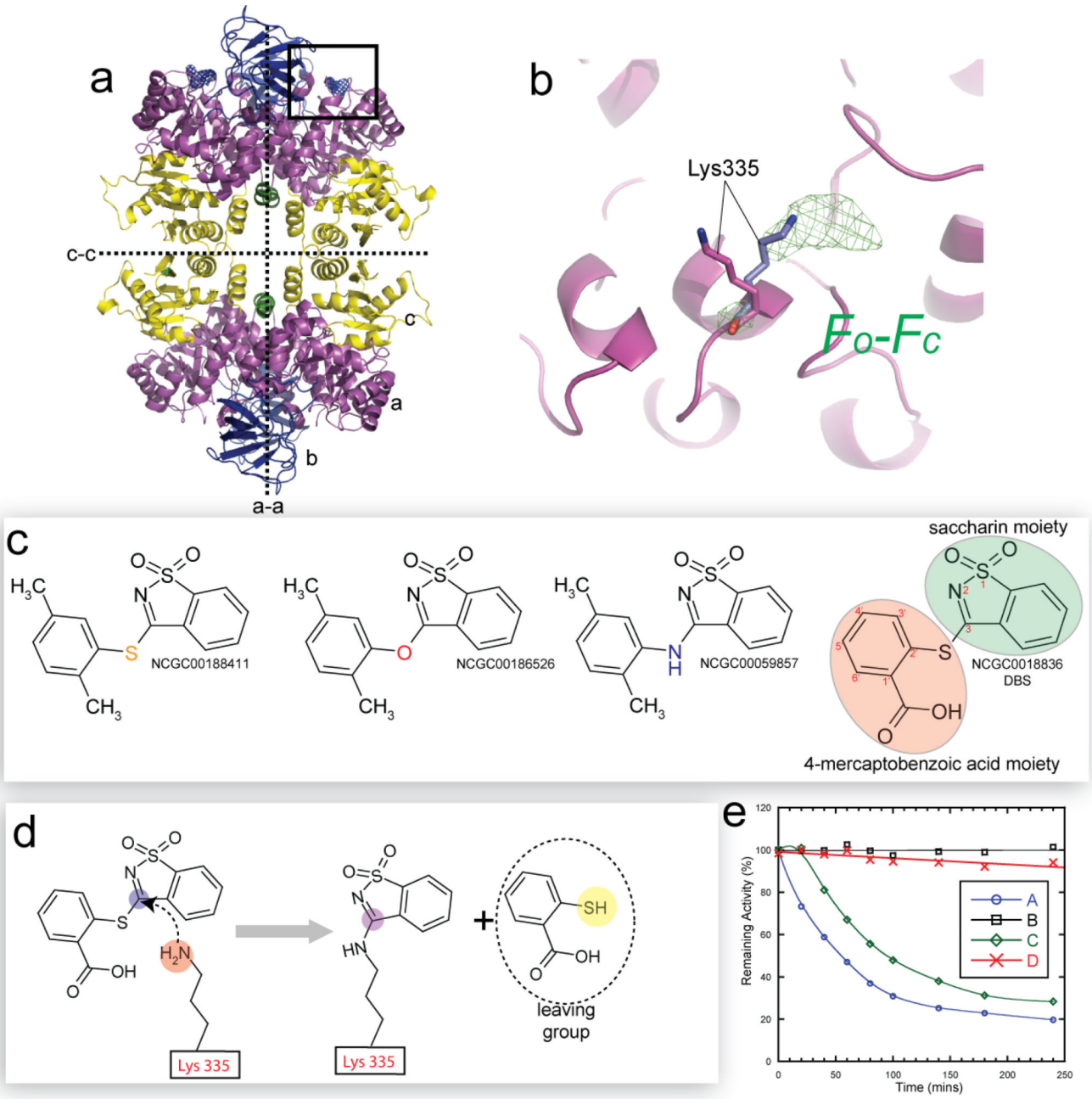

Figure 1. Proposed reaction mechanism of DBS

(**a**) The four-domain structure of *Lm*PYK-OX/DBS is indicated by different colours: green, short N-terminal domain; purple, domain A, blue; domain B; yellow, domain C. The large (a-a) and small (c-c) subunit interfaces are indicated by dotted lines. The black box designates the position of the active site of one subunit, and is shown in close up in panel b. (**b**) The difference (F_o-F_c map shown in green at a resolution of 3.5 Å, contoured to 2.5 σ) electron density observed in all four active sites is associated with Lys335 in a novel orientation (blue). (**c**) Two-dimensional structures of (NCGC00188411), (NCGC00186526) (NCGC00059857) qHTS compared with the structure of the synthesised analogue NCGC00188636 (DBS) that displayed enhanced stability and solubility. (**d**) The proposed reaction mechanism for the covalent modification of Lys335. (**e**) Time-dependent inhibition

of LmPYK by pre-incubation with 50 μM DBS under variable conditions. (A) LmPYK pre-incubated with 0.4 mM PEP and 50 μM DBS. (B) LmPYK pre-incubated with 0.4 mM PEP (no inhibitor). (C) LmPYK pre-incubated with 0.4 mM PEP, 4 μM F26BP and 50 μM DBS. (D) LmPYKΔK335R pre-incubated with 0.4 mM PEP and 50 μM DBS.

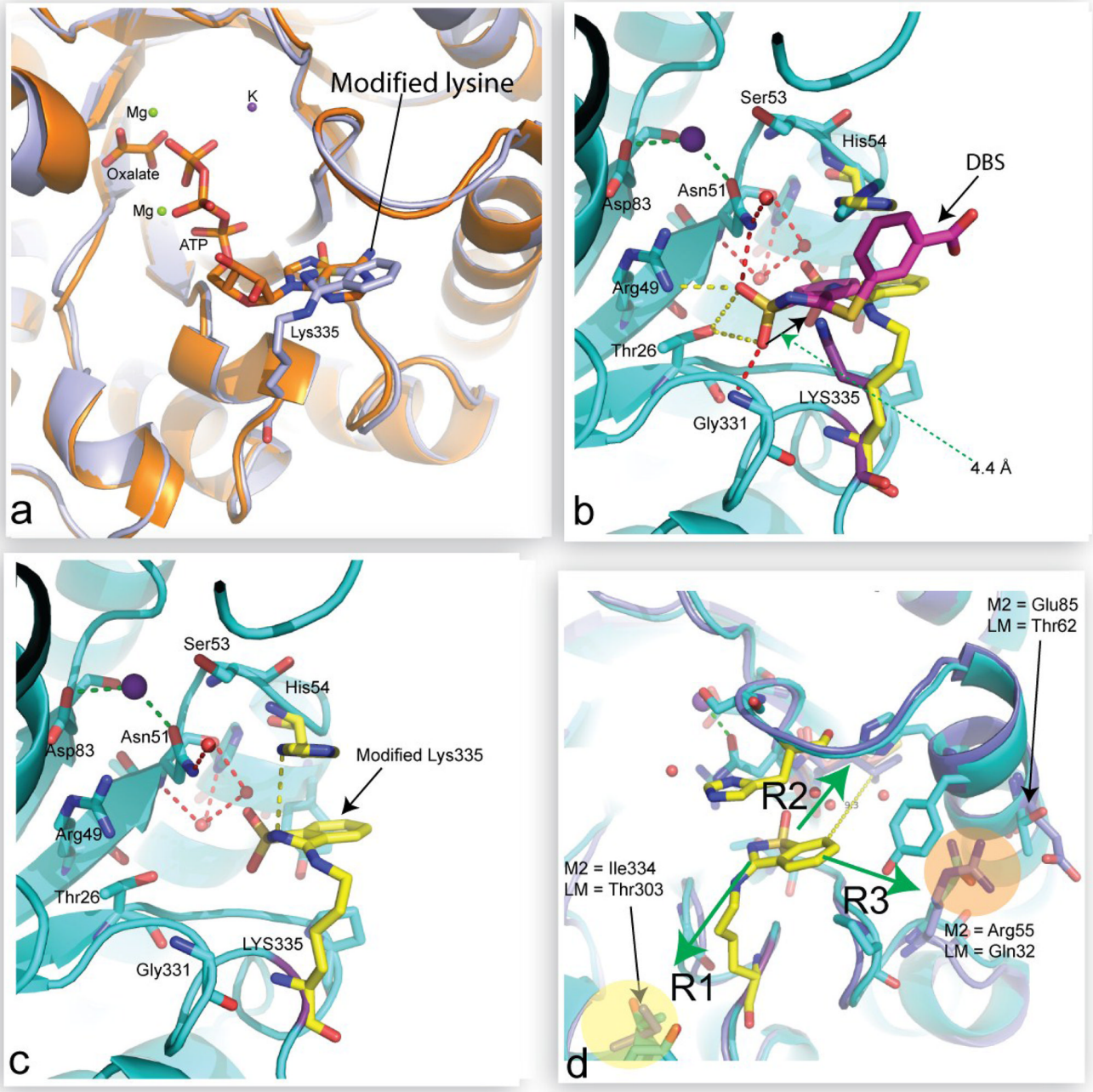

Figure 2. DBS reacts with Lys335 at the active site of *Lm*PYK

All ligands and interacting amino-acid residues are shown as sticks, and waters as red spheres. (**a**) The superpositions of the ATP and the modified Lys335 indicate that the ATP/ADP binding may be sterically hindered. (**b**) The proposed position of Lys335 prior to covalent modification is shown by purple sticks. Initially the sulphur dioxide group of the DBS molecule (pink sticks) binds to the active site, occupying a similar position to the sulphono group of suramin (*Lm*PYK-suramin structure [15], see Supplementary Figure S4). The network of interactions (dashed red line = interactions <3 Å, dashed yellow lines = interactions 3–4 Å, dashed green lines = coordination of the inorganic cations) hold DBS in

place, providing an ideal reactive geometry for the reaction with Lys335 to occur. (**c**) Final refined position of covalently modified Lys335 as observed in the crystal structure. (**d**) Overlay of the X-ray structures of *Lm*PYK (this paper) and the X-ray structure of *Hs*M2PYK showing differences in the amino acid side chains in three regions (R1, R2 R3) around the modified Lys335 (yellow) that could enable the design of isoenzyme-specific families of inhibitors.

Table 1

Data collection and refinement statistics

Values in parentheses are for the highest-resolution shell.

Data collection	
Space group	I222
Cell dimensions	
a, *b*, *c* (Å)	122.4 , 130.2, 166.5
Solvent content (%)	60.00
Wavelength (Å)	0.98
Resolution (Å)	60.85-2.65 (2.79-2.65)
R_{sym}	0.09 (0.64)
I / σ(I)	8.3 (1.7)
Completeness (%)	98.0 (98.8)
Redundancy	2.8 (2.8)
Refinement	
Resolution (Å)	60.85-2.65
No. reflections	35936
R_{work} / R_{free}	22.3/26.6
Average protein *B*-factor (Å^2)	31.4
No. Residues	894
R.m.s. deviations	
Bond lengths (Å)	0.01
Bond angles (°)	0.90